International Journal of Thermofluid Science and Technology (2019)
Vol. 6, No. 4, Paper No. 19060403
https://doi.org/10.36963/IJTST.19060403
Research Article

Fluid Flow and Heat Transfer Characteristics of Multiple Swirling Impinging Jets at Various Impingement Distances

Md Habib Ullah Khan*, Zahir U. Ahmed

Department of Mechanical Engineering, Khulna University of Engineering & Technology, Khulna-9203, Bangladesh

Received: 18 March 2019; Received in revised form: 20 May 2019; Accepted: 19 August 2019; Published online 10 September 2019

Abstract

This research investigates the fluid flow and heat transfer characteristics for the effect of multiple swirling jets impinging on a heated plate. In this regard, numerical simulations were performed for the inline-type jet arrangement using ANSYS v16.2. Governing equations for turbulent swirl flows were solved by coupled algorithm whereby turbulences are described by SST k-ω model. The analysis is studied for Reynolds number Re = 11600 and swirl number 0.74 at impingement distances equal to 1, 2, 3 and 4 times nozzle diameter. The numerical results showed that impinging distance has a significant effect on both heat transfer and fluid flow characteristics. In case of low impinging distance (H=1D) swirling effect was dominant and the strong recirculation zones resulted in a higher heat transfer from the heated surface. With the increase of impingement distance, the turbulent kinetic energy reduced significantly near the heated surface. It was evident that for higher impingement distance (H=4D) the effect of swirl was greatly reduced resulting in a lower heat transfer from the heated surface.

Keywords: CFD, Heat Transfer, Impinging Jet, Swirl, Turbulence.

1. Introduction

Impinging jets are widely used in cooling and heating applications. Moderate heat transfer rate of impinging jets increased its applications substantially and also gained popularity among researchers. Impinging jet is used in gas turbine cooling, electrical equipment cooling, heating and also in textile industries. There are several factors which affect the heat transfer rate of impinging jets and complicate the phenomena. Zerrout et al. (2016) reported for a three swirling jet system that different jet configuration and impingement distance is significant for heat transfer of swirling impinging jet. Terekhov et al. (2018) alalyzed impinging jet flow for low Reynolds number and stated that maximum heat transfer occurs for low Reynolds number. So, among the factors

*Corresponding e-mail: habibullahkhan@me.kuet.ac.bd

Reynolds number, jet diameter, impingement distance, jet-to-jet distance are found to be the important and may potentially alter fundamental behaviors when swirl is added to an impinging jet, which is the primary focus of the current study. In addition, Xu et. al. (2017) reported that thermal stress generated by non-uniform heating or cooling by conventional (non-swirl) impinging jet may induce rupture of the structure from excess stress generation. As such, it warrants further research so as to uniform heating or cooling can be achieved. To this connection, Markal (2018) performed experimental investigation on swirling co-axial impinging jet and found that better uniform heat transfer occurs with the increase of flow rate. This observation agrees with the previous experimental study on aerodynamic swirling jets by Ahmed et al. (2016), who also speculated more uniform heat transfer only at moderate swirling impinging jet. However, such uniformity in heat transfer is also significantly dependent on the impingement distance. So, further research on strong swirling jets or multiple swirling impinging jets may be required to improve the uniformity of heat transfer on the impingement surface.

Existing literature includes investigations mainly on non-swirling impinging jets both for single jet or multiple jets. In contrast, multiple swirling impinging jets are very limited in the literature. Several swirl generating mechanisms had previously been tested for single jets, for example using geometric means i.e. twisted tape and block inserts, and aerodynamic. Nuntadusit et al. (2012) experimentally studied the effect of nozzle-to-nozzle distance in geometric swirling jets and found that multiple swirling jets provided higher heat transfer rate than conventional (non swirl) impinging jets. Again, Amini et al. (2015) numerically studied different jet-to-plate distance and twist ratios of inserts and found that for low impingement distance (H/D=2) swirling impinging jets provided lower heat transfer rate than conventional impinging jets. The opposing behaviors for geometrically generated swirl may be due to the variations of jet inlet from the swirl generating mechanisms and different impingement distance, which influences fluid interactions. Marzec and Pietal (2014) studied the effect of different nozzle geometries and found that installing features between adjacent jets may redirect the flow and improve the heat transfer characteristics for impinging jets. Recently, Ahmed et al. [2016] found single swirling jet is detrimental to surface heat transfer, particularly at larger impingement distances (H/D> 3). Several researchers suggested that single swirling impinging jets has benefit in terms of heat transfer intensity and uniformity over their non-swirling counterpart at higher impingement distances. At lower impingement distances, higher heat transfer rate is observed with the expense of large non-uniformity. Lee et al. (2002) suggests that the effect of single swirl is found to be beneficial only for a jet-to-plate distance (H/D=2) and for higher impingement distances the benefit of swirl flow is not evident. The likely jet-to-jet interactions in multiple swirling jets may affect such characteristics, as will be seen in the ensuing study.

Ianiro and Cardone (2012) showed that multichannel nozzles have higher heat transfer at all impingement distances than single nozzle and have relatively higher peak at a lower jet-to-plate distance (H/D=2). They also reported that for non-swirling multichannel flow the heat transfer rate increases up to H=8D distance whereas the heat transfer rate of swirling jets decreases with an increase of the nozzle-to-plate distance.Aldabbagh and Sezai (2002) reported that for multiple impinging jets a peripheral vortex is generated around each jet and an up-wash fountain is also generated. He reported that the heat transfer is significantly affected by the nozzle-to-plate distance and jet-to-jet spacing doesn't significantly affect heat transfer.Draksler et al. (2017) reported for multiple impinging jets in hexagonal configuration that jet-to-jet spacing of (s/D=2) helps to retain the characteristics of single impinging jet and the development of the fluid flow interactions alike it.

It appears that previous research on impinging jet is highly focused for conventional (non-swirling) single and multiple jets as well as single swirling jets, both aerodynamic (axial-plus-tangential flow mixing) and geometric (vane, inserts etc.). Relatively limited studies on multiple swirling jets are available in the literature whereby swirl is generated geometrically in majority of these studies. Some studies reported that such geometry-induced swirling jets are known to have negative impacts on heat transfer due to the inherent bluff-body, lack of control on swirl intensity and strong dependency of results on geometrical shape. As such, aerodynamic swirling jets may be considered to elucidate the exact effect of swirl on flow behaviors for multiple impinging jets, as investigated in this study. In this regard, numerical investigation is carried out to examine the fluid flow and heat transfer characteristics for various swirl intensities at a Reynolds number equal to 11,600 and the range of impingement distance 1D-4D.

Nomenclature

D	diameter of the nozzles (40 mm)	h	heat transfer Co efficient (W/m^2K)
H	nozzle to plate Distance (mm)	r	radial co ordinate (mm)
q	joule Heating (W/m^2)	A	area of the impingement surface (m^2)
N_u	local Nusselt Number (Dimensionless)	Z	axial co ordinate (mm)
$\bar{N}_u$	spatially averaged Nusselt number	X	ordinate of the impingement plane (mm)
S	swirl Number (Dimensionless)	Y	abscissa of the impingement plane (mm)
R_e	Reynolds Number (Dimensionless)	U_c	velocity along centerline (m/s)
T_w	heated wall temperature	U_b	bulk velocity (m/s)

2. Numerical Methodology

Steady incompressible turbulent swirling impinging air jets are solved using RANS equations for mass, momentum and energy conservations. The generalized RANS equation for flow field and heat transfer is obtained as (Ahmed et al., 2017):

$$\frac{\partial(\rho u\phi)}{\partial x}+\frac{\partial(r\rho v\phi)}{r\partial r}=\frac{\partial}{\partial x}(\Gamma_\phi\frac{\partial\phi}{\partial x})+\frac{\partial}{r\partial r}(r\Gamma_\phi\frac{\partial\phi}{\partial r})+S_\phi \quad (1)$$

where, ϕ , Γ_ϕ and S_ϕ represents the generalized variables, effective transport coefficients and source terms respectively. Different variables, effective transport coefficients and source terms used in the governing equations are available in Ahmed et al. (2017), and hence is not reported here for brevity.

The turbulence closures associated with RANS approach are achieved via mean velocity gradients by the Boussinesq hypothesis using eddy viscosity and eddy thermal conductivity. The eddy transport coefficients are solved by SST k-ω turbulence model, which is considered to be effective for the prediction of near wall turbulence region. The Shear Stress Transport (SST) k-ω model by Menter and Egorov (2010) is:

$$\frac{\partial}{\partial t}(\rho k)+\frac{\partial}{\partial x_i}(\rho k u_i)=\frac{\partial}{\partial x_j}(\Gamma_k\frac{\partial k}{\partial x_j})+\tilde{G}_k-Y_k+S_k \quad (2)$$

$$\frac{\partial}{\partial t}(\rho\omega)+\frac{\partial}{\partial x_i}(\rho\omega u_i)=\frac{\partial}{\partial x_j}\left(\Gamma_\omega\frac{\partial\omega}{\partial x_j}\right)+G_\omega-Y_\omega+D_\omega+S\omega \quad (3)$$

In these equations $\tilde{G}_k$ and G_w represent the generations of turbulence kinetic energy due to mean velocity gradients and specific dissipation rate ω. Γ_k and Γ_ω represent the effective diffusivity of k and ω respectively. Y_k and Y_ω represent the dissipation of k and ω due to turbulence. D_ω represents the cross diffusion term, and S_k and S_ω are user defined source terms. Detailed expressions of these terms are available in the Table 1 of Ahmed et al. (2017).

A finite-volume based software ANSYS Fluent v16.2 was used to solve the mean and turbulence quantities. An inline array of 17 circular nozzles with the same diameter D equally positioned (45^o interval) in two circles (8 each) and one in the center is considered in this study. Inner and outer circle is located at a distance of 2D and 4D, respectively from the center. Swirling jets generated by any means emanated from these nozzles and impinges on a flat smooth surface located at a distance H. A quarter of the full 3-D model was considered for simulation due to the symmetric nature and to

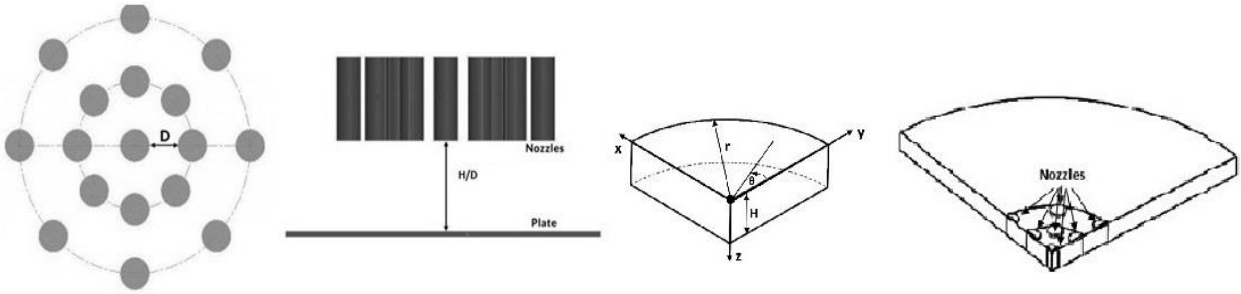

Fig. 1. Physical set up of the system

save the computational cost. The relative position of the nozzles, physical setup of the geometry and the numerical domain is shown in Figure 1. The radial extent of the numerical domain was sufficiently large i.e. 15D from the center to avoid the end effect to the region of interest. The pressure velocity coupling was implemented using the coupled solver algorithm with Green-Gauss Cell spatial discretization for gradients, PRESTO for pressure and second order upwind scheme was used for momentum, turbulent kinetic energy, specific dissipation rate and energy. All the residuals were set to 10^{-5} for accuracy except energy to 10^{-6}.

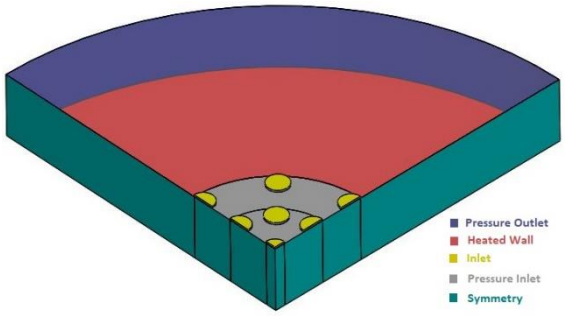

Fig. 2. Solution Domain and Boundary Conditions

Unstructured triangular mesh is used with inflation at the impingement surface whereby 15 layers with growth rate of 1.2 is applied to capture near wall behaviors well. Fine mesh was generated near the axis and progressively coarser mesh in the radially outward direction. Mesh independency was performed with three mesh elements, namely 330470, 470010 and 596019, and the mesh consisting of 470k elements was found to be sufficient to predict numerical results, as increasing to higher mesh elements does not alter the results remarkably.
Inlet conditions for the numerical simulation is taken from an experimental study of single swirling impinging jets where swirling is achieved by a nozzle that has the ability to provide non-swirling-to-strongly swirling jets for the same flow rate (Ahmed et al. 2016). Introducing data from such swirl nozzle may help to see the exact scenario for the effect of multiple swirling jets on thermofluidic behaviors. Mean and turbulence quantities at the exit of the single swirl nozzle (Ahmed et al. 2016) were taken as the inlet in the current simulation. In this regard, experimental data for axial velocity (u) and tangential velocity (w) component as well as k and ω for a single jet is used for all nozzles. The fluid inlet temperature is set to ambient (300 K). Outlet boundary was set as pressure outlet. Periodic boundary conditions were applied at the two side surfaces of the domain, which were patch-controlled during meshing in order to impose periodic boundary. No slip boundary is applied at the impingement surface with constant heat flux equal to 1070 W/m^2, similar to the experimental conditions.

The swirl intensity is characterized by swirl number and the definition is similar to the experimental study (Ahmed et al. 2016) for consistency:

$$S=\frac{W_b}{U_b}, \tag{4}$$

where U_b and W_b are the bulk axial and tangential velocity, determined by averaging velocity profiles across the nozzle diameter at the swirl nozzle exit as:

$$U_b=\frac{2}{R^2}\int_0^R urdr \tag{5}$$

and

$$W_b=\frac{2}{R^2}\int_0^R wrdr \tag{6}$$

In this study, a swirl number S = 0.74 is considered that corresponds to a strong swirling jets where both axial and tangential velocities increases with radius and have a peak near the wall. Further detail of the profiles and explanations is available in Ahmed et al., 2016. The local heat transfer coefficient h and Nusselt number are defined by:

$$h=\frac{q}{T-T_W} \tag{7}$$

$$Nu=\frac{hD}{k_{air}} \tag{8}$$

In these equations T_w is the wall temperature, q is the net heat flux of the plate and k_{air} is the thermal conductivity of the impinged air. The skin friction coefficient is defined by:

$$C_f=\frac{\tau_w}{\frac{1}{2}\rho U_b^2} \tag{9}$$

where τ_w is the wall shear stress.

The current simulation is first validated against published literature (Tummers et al. 2004, Fairweather et al. 2002, Geers et al. 2004, Ahmed et al. 2016) for single jet. Fig. 3 presents the axial

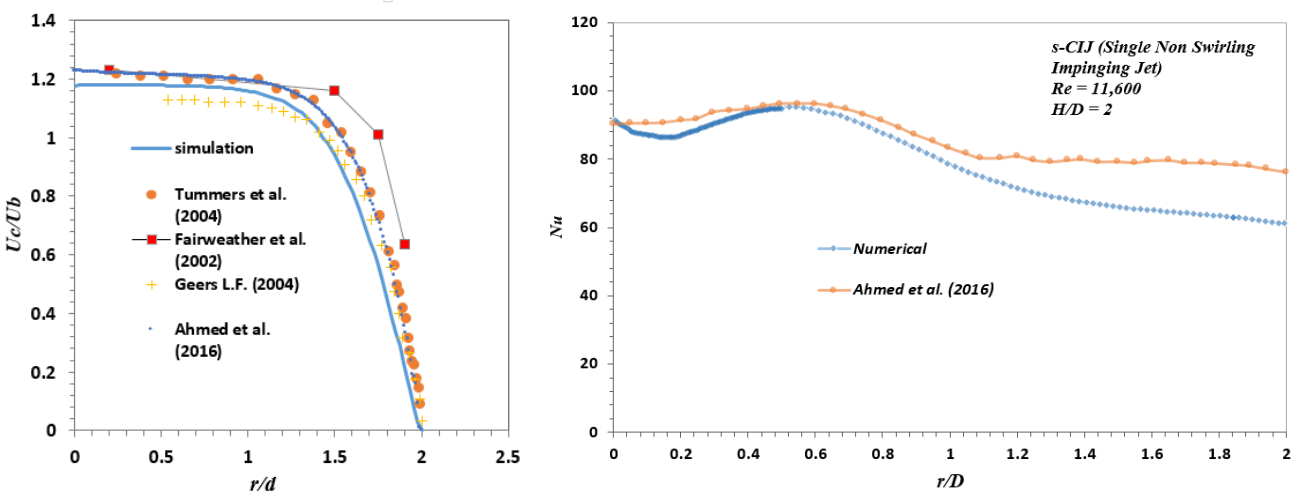

Fig.3. Comparison between the current result and experimental data for velocity and heat transfer distribution.

velocity (left) along the axis U_c (r=0, z) for H/D = 2 case and radial distribution of heat transfer (right) within r/D ≤ 2.0. The centerline velocity U_c is normalized by U_b . This bulk axial velocity is also used to calculate Reynolds number. The results generally are in good agreement with each other. The slight deviations among the velocity profiles may be due to the variations of different inlet boundary conditions, different nozzle diameters and plate dimensions. Similar to the velocity profiles, a good agreement is also found for Nu distribution and its magnitude, with a deviation from the experimental data at r/D > 1.5. This may be due to the intense flow mixing and turbulence in that region. Both velocity and heat transfer validation with existing literature showed the reliability and accuracy of the current simulation methodology.

3. Results and Discussions

3.1 Flow Field Characteristics

Fig.4 presents the velocity streamline of array of swirling impinging jet at a symmetric plane y=0 for various impingement distances H/D = 1, 2, 3 and 4. It is evident from the figure that several recirculation zones appear between two neighboring jets and around the each jet axis, with a strong recirculation around the central jet axis. For the smallest distance (H/D = 1), such recirculation zones had strong appearance, due to the jets have little space to move away and their interactions induce recirculation. It is worth noting here fountain creation with an upward movement due to the interaction of non-swirling jets (Geers et al., 2004) does not exist in swirling impinging jets. As the H/D ratio increases, it is found that these recirculation zones become weaker eventually tends to disappear for the highest H/D investigated, except the recirculation zone near the impingement surface around the central jet axis. The extent of which becomes larger with the increase of H/D. This is attributed to the tangential components of the jet which tends to move the fluid stream

radially away with the increase of H. This causes a larger adverse pressure region around the jet axis. Beyond r = 5D, streamlines seem to have similar behavior regardless of the impingement distance, and sweep away in radial direction. It may be presumed from the results that due to decreased turbulence at higher H/D ratio the heat transfer rate may decrease accordingly.

Fig.5 shows the pressure distribution on the impingement surface at various H/D. The same color scale is used for all the results to facilitate better explanations. The static pressure is found to be stronger only in the impingement region for the smallest H/D and more uniformly distributed at higher H/D. For small H/D, the jet has the maximum kinetic energy which essentially converts into pressure, and as the H/D increases fluid streams becomes weaker and spreads out. For conventional (non-swirling) impinging jet this uniform pressure distribution is not evident.

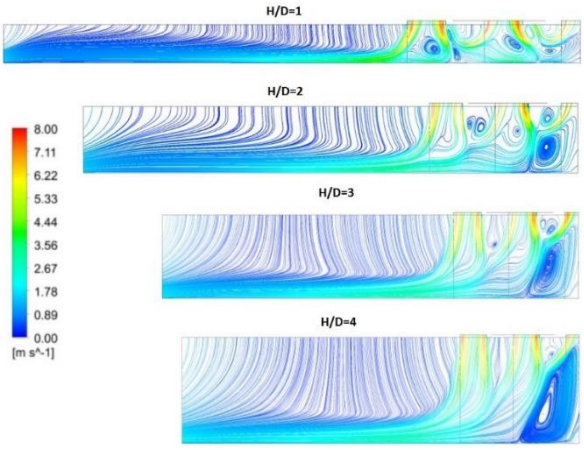

Fig.4. Velocity Streamline for different H/D ratio at S=0.74

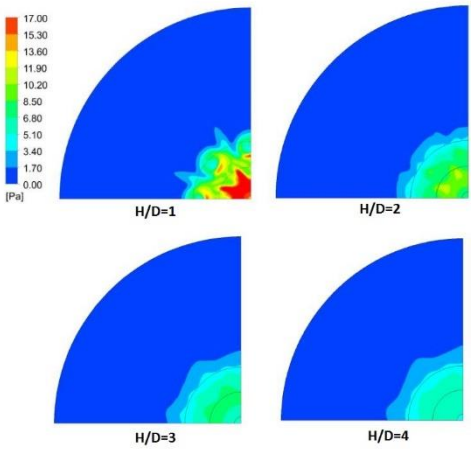

Fig.5. Pressure contour for different H/D

Fig. 6 compares the co-efficient of skin friction (C_f) along any radial direction for various impingement distances (H=1D-4D). It appears that three maximum peaks around 1.5D, 3.5D and 5.1D occur for the lowest impingement distance H/D=1. The first two peaks appear to be correlated

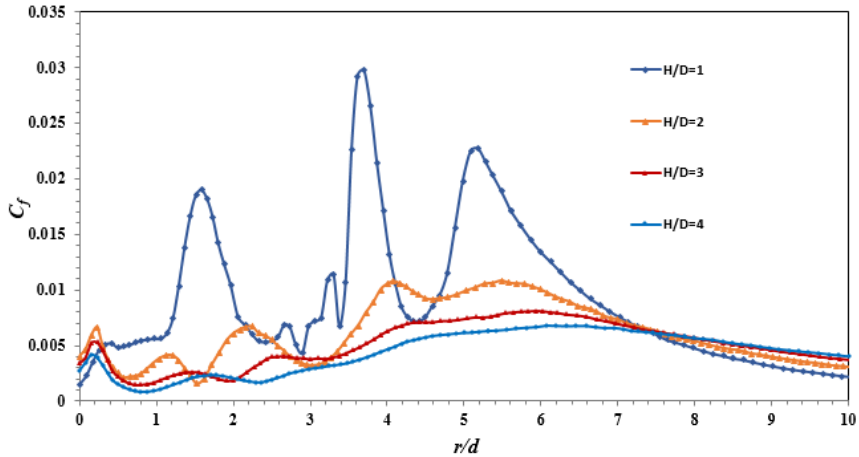

Fig. 6. Co-efficient of skin friction distribution at various H/D for swirling jets

with corresponding recirculation in those regions. Strong radial flows exist near the impingement surface underneath these recirculation zones, which may be the reason for the first two peaks. The third peak, however, resembles to the strong shear layer and mixing zones for a single swirling jets. With the increase of the impingement distance the peaks becomes weaker and tends to shift radially outward, which is correlated with the jets movement when H increases. The distributions for H/D=3 and H/D=4 are almost identical in nature and less significant in magnitude. This aspect corroborates well with the similar velocity streamline characteristics at these two distances.

Eddy turbulent viscosity (μ_t) is the key parameter in defining turbulence for two-equation models. As such, Fig. 7 presents the contour of eddy viscosity ratio (μ_t / μ) along the symmetric plane (y=0) for various H/D distances. At the smallest H/D, eddy viscosity confined to the jet interaction regions only, as at this distance the jets have minimum space to mix further before impingement. With the increase of H/D, the extent of the mixing region becomes larger and fluids streams interacts intensely, which is evident from the figures for H/D = 2-4, where eddy viscosity ratio significantly increases with H and near the impingement surface. A very weak viscosity ratio appears near the surface around central axis for all H, which is attributed to the lack of fluid streams in that region.

Fig. 8 represents the turbulent kinetic energy, another important turbulence parameter, for swirling impinging jets at various H/D. The turbulent kinetic energy appears to be strong at small impingement distances, such as H/D =1 and 2. With the increase of impingement distance, turbulence is found to be scattered outward limiting its intensity. The effect of jet interaction is also found strong at small impingement distance. This aspect may significantly affect heat transfer, which will be discussed in the ensuing results.

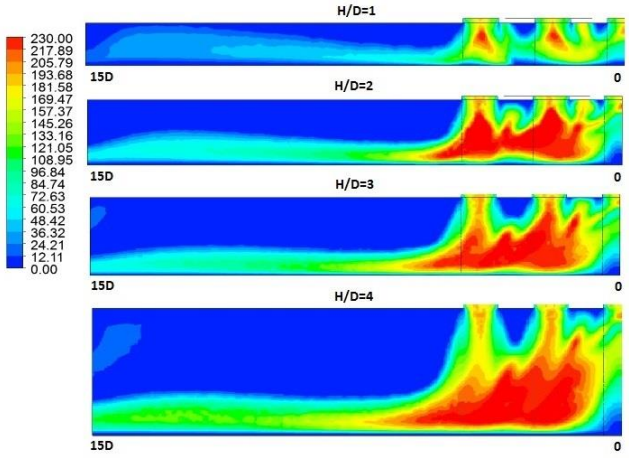

Figure 7 Effect of impingement distance on eddy viscosity ratio at S = 0.74.

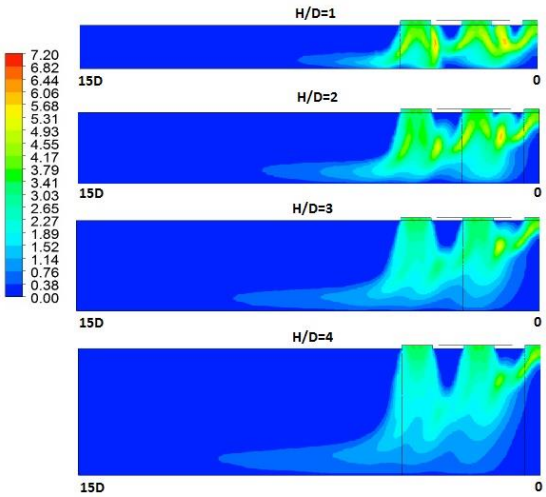

Figure 8 Turbulent Kinetic Energy for the effect of H/D at the same swirl and Reynolds number.

3.2 *Heat Transfer Characteristics*

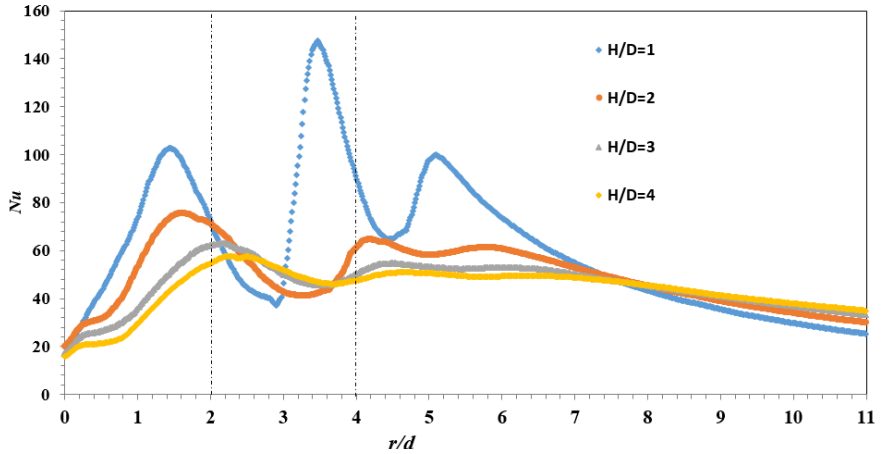

Fig. 9. Local Nusselt number distribution for different H/D ratio at S=0.74

Fig. 9 depicts the local Nusselt number distribution along radial direction at the symmetric plane (y=0) on the impingement surface. The radial location of nozzle axis is also shown in the figure by vertical dotted line. It shows that heat transfer is minimum at the central axis (r = 0) region and maximum between the neighboring nozzles. Similar to the skin friction coefficient profiles at H/D =1, three peaks also appear at the similar radial locations i.e. 1.5D, 3.5D and 5.1D, which may be due to the strong radial flow corresponding to recirculation zone near the surface at those locations that causes increased heat transfer. At higher H/D, such similarities do not exist, and the number of peak reduces to two for H/D =2 and to one for H/D=3,4. Within the first two nozzles heat transfer is decreasing with the increasing H/D, which may be associated with the reduced velocity due to the larger travel distance of the jets. The peak Nu shifts radially away with the increase of H/D. The effect of H/D is found to be insignificant on local Nusselt number distribution beyond r/D=7.

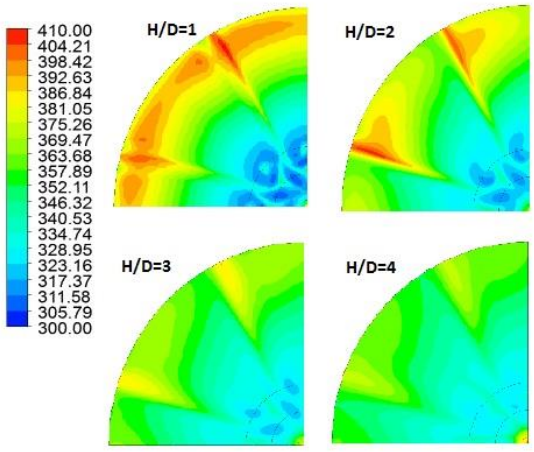

Fig. 10. Temperature Contour for various impingement distance

Fig. 10 shows the temperature contour of the heated impingement plate for different H/D. It is

evident from the figure that maximum cooling was obtained for the lowest impingement distance below the nozzles and between the nozzles where a strong recirculation region exists. As the impingement ratio increases the temperature distribution of the wall becomes more uniform and cooling effect extends radially farther. It appears that there is a competition between the cooling and uniformity of heat transfer. The uniformity is achieved by the expense of cooling effect.

Finally, Fig. 11 presents the area-averaged Nusselt number for the swirling flows at various H/D. For H/D=1, the heat transfer is found to be larger than other impingement distances, i.e. H/D=2,3,4 with a percentage improvement of 29.58%, 53.8%, 71.27%, respectively. This result appears to be

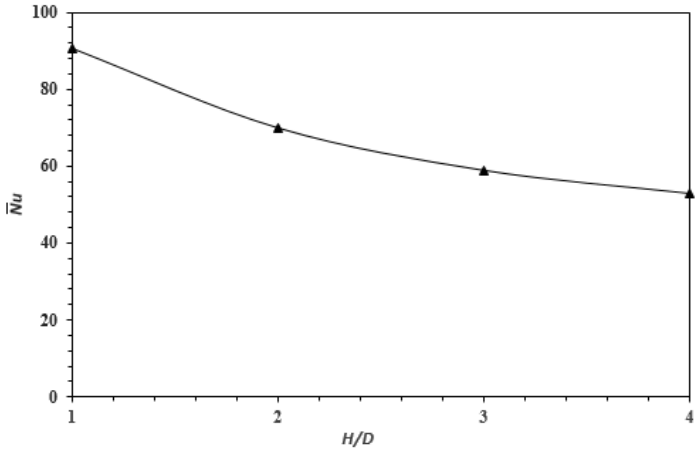

Fig. 11. Average Nusselt Number distribution for different H/D ratio at S=0.74

consistent with other results of this study. At higher impingement distance, kinetic energy of the jet and turbulence becomes weaker, and consequently less heat transfer occurs.

4. Conclusion

A numerical analysis is carried out to investigate the flow field and heat transfer characteristics of turbulent multiple swirling jets when strong swirl (S=0.74) is imposed through the nozzle at different impingement distances within the range H/D=1-4 at Reynolds number Re=11,600. In this case, RANS equations are solved coupled with SST k-ω turbulence closure via ANSYS Fluent v16.2. The results show that several recirculation zones appear between jets and the impingement surface that are found to be significant in fluid flow and heat transfer behaviors. For the smallest distance (H/D = 1), such recirculation zones had strong appearance, and they become weaker as H/D increases and eventually tends to disappear for the highest H/D, except the recirculation around the central axis which becomes larger with the increase of H/D. The static pressure is found to be stronger only in the impingement region for the smallest H/D and more uniformly distributed at higher H/D. Few peaks of skin friction coefficient is also predicted for H/D=1 which are found to be correlated with heat transfer peaks. With the increase of the H/D the peaks becomes weaker and tends to shift radially outward. As expected, better turbulence and flow mixing is achieved at higher H/D. A non-uniform but highly improved heat transfer is obtained at the smallest H/D, but relatively more uniform with reduced magnitudes is predicted at higher H/D.

References

Ahmed, Z. U., Al-Abdeli, Y. M., and Guzzomi, F. G., (2017). Flow field and thermal behaviour in swirling and non-swirling turbulent impinging jets, International Journal of Thermal Sciences, vol. 114, pp. 241-256.

Ahmed, Z. U., Al-Abdeli, Y. M., and Guzzomi, F. G., (2016). Heat transfer characteristics of swirling and nonswirling impinging turbulent jets, International Journal of Heat and Mass Transfer, vol. 102, pp. 991-1003.

Ahmed, Z. U., (2016). An Experimental and Numerical Study of Surface Interactions in Turbulent Swirling Jets, PhD Thesis, Edith Cowan University, Joondalup, Australia.

Ahmed, Z. U., Al-Abdeli Y. M., and Matthews, M. T., (2015). The effect of inflow conditions on the development of non-swirling versus swirling impinging turbulent jets, vol. 118, Computers &Fluids, pp. 255-273.

Ahmed, Z. U., Al-Abdeli, Y. M.,and Guzzomi, F. G., (2015). Impingement pressure characteristics of swirling and non-swirling turbulent jets, Experimental Thermal and Fluid Science, Vol.68, PP.722-732.

Aldabbagh, L.B.Y., Sezai, I., (2002). Numerical simulation of three-dimensional laminar multiple impinging square jets, International Journal of Heat and Fluid Flow, 23, 509–518.

Caicedo, J. M., Marulanda, J., Thomson, P., and Dyke, S. J. (2001). Monitoring of bridges to detect changes in structural health. In American Control Conference, Proceedings of the 2001 (Vol. 1, pp. 453-458). IEEE.

Constantinides, A., and Mostoufi, N. (1999). Numerical methods for chemical engineers with MATLAB applications. Upper Saddle River, NJ: Prentice Hall PTR.

Draksler, M., Koncar, B., Cizelj, L., Niceno, B., (2017). Large Eddy Simulation of multiple impinging jets in hexagonal configuration – Flow dynamics and heat transfer characteristics, International Journal of Heat and Mass Transfer, 109, 16–27.

Fairweather, M., and Hargrave, G., (2002). Experimental investigation of an axisymmetric, impinging turbulent jet. 1. Velocity field, Experiments in Fluids, vol. 33(3), pp. 464-471.

Geers, L. F., Tummers M. J. and Hanjalic´ K., (2004). Experimental investigation of impinging jet arrays, Experiments in Fluids, vol. 36(6), pp. 946-958.

Geers, L. F., (2004) Multiple impinging jet arrays: an experimental study on flow and heat transfer, PhD Thesis, Technical University, Delft , The Netherlands.

Ianiro, A. and Cardone, G., (2012). Heat transfer rate and uniformity in multichannel swirling impinging jets, Applied Thermal Engineering, 49, 89-98.

Lee, D. L., Won, S. Y., Kim, Y. T. and Chung, Y. S., (2002). Turbulent heat transfer from a flat surface to a swirling round impinging jet, International Journal of Heat and Mass Transfer 45, 223-227

Markal, B. (2018). Experimental investigation of heat transfer characteristics and wallpressure distribution of swirling coaxial confined impinging air jets, International Journal of Heat and Mass Transfer 124 (2018) 517–532

Marzec, K., Kucaba-Pietal, A., (2014). Heat transfer characteristic of an impingement cooling system with different nozzle geometry, K Marzec and A Kucaba-Pietal 2014 J. Phys.: Conf. Ser. 530 012038

Menter F. and Egorov Y., (2010), The Scale-Adaptive Simulation Method for Unsteady Turbulent Flow Predictions. Part 1: Theory and Model Description. Journal Flow Turbulence and Combustion. 85. 113–138.

Nuntadusit C., Wae-hayee M., Bunyajitradulya A., Eiamsa-ard S., (2012). Heat transfer enhancement by multiple swirling impinging jets with twisted-tape swirl genera-tors, International Communications in Heat and Mass Transfer, Vol. 39 (1), PP. 102-107.

Vadim V. Lemanov, Viktor I. Terekhov, Vladimir V. Terekhov., (2018). Heat transfer of impinging jet at low reynolds number, International Heat Transfer Conference 16, Volume 14, 2018, Heat Transfer Enhancement, DOI: 10.1615/IHTC16.hte.023057, pages 5501-5508

Xu, L., Lan, J., Ma, Y., Gao, J., Li, Y., (2017).Numerical study on heat transfer by swirling impinging jets issuing froma screw-thread nozzle, International Journal of Heat and Mass Transfer, Volume 115, Part A, December 2017, Pages 232-237

Younes Amini, Mojtaba Mokhtari, Masoud Haghshenasfard, Mostafa Barzegar Gerdroodbary, (2015). Heat transfer of Swirling Imping-ing Jets Ejected from Nozzles with Twisted Tapes Utilizing CFD Technique, Case Studies in Thermal Engineering, Vol. 6, PP. 104-115.

Zerrout A., Khelil A. and Loukarfi L., (2016). Numerical study of a three swirling jets system impacting a plane plate, Mechanics & Industry 18, 103 (2017) (c) AFM, EDP Sciences 2016